

# UC San Diego

## UC San Diego Previously Published Works

### Title

LRP1 Has a Predominant Role in Production over Clearance of A $\beta$  in a Mouse Model of Alzheimer's Disease.

### Permalink

<https://escholarship.org/uc/item/9m47164c>

### Journal

Molecular neurobiology, 56(10)

### ISSN

0893-7648

### Authors

Van Gool, Bart  
Storck, Steffen E  
Reekmans, Sara M  
et al.

### Publication Date

2019-10-01

### DOI

10.1007/s12035-019-1594-2

Peer reviewed



# LRP1 Has a Predominant Role in Production over Clearance of A $\beta$ in a Mouse Model of Alzheimer's Disease

Bart Van Gool<sup>1</sup> · Steffen E. Storck<sup>2</sup> · Sara M. Reekmans<sup>1</sup> · Benoit Lechat<sup>1</sup> · Philip L. S. M. Gordts<sup>1,3</sup> · Laurent Pradier<sup>4</sup> · Claus U. Pietrzik<sup>2</sup> · Anton J. M. Roebroek<sup>1</sup>

Received: 23 January 2019 / Accepted: 2 April 2019 / Published online: 19 April 2019  
© The Author(s) 2019

## Abstract

The low-density lipoprotein receptor-related protein-1 (LRP1) has a dual role in the metabolism of the amyloid precursor protein (APP). In cellular models, LRP1 enhances amyloid- $\beta$  (A $\beta$ ) generation via APP internalization and thus its amyloidogenic processing. However, conditional knock-out studies in mice define LRP1 as an important mediator for the clearance of extracellular A $\beta$  from brain via cellular degradation or transcytosis across the blood-brain barrier (BBB). In order to analyze the net effect of LRP1 on production and clearance of A $\beta$  in vivo, we crossed mice with impaired LRP1 function with a mouse model of Alzheimer's disease (AD). Analysis of A $\beta$  metabolism showed that, despite reduced A $\beta$  clearance due to LRP1 inactivation in vivo, less A $\beta$  was found in cerebrospinal fluid (CSF) and brain interstitial fluid (ISF). Further analysis of APP metabolism revealed that impairment of LRP1 in vivo shifted APP processing from the A $\beta$ -generating amyloidogenic cleavage by beta-secretase to the non-amyloidogenic processing by alpha-secretase as shown by a decrease in extracellular A $\beta$  and an increase of soluble APP- $\alpha$  (sAPP- $\alpha$ ). This shift in APP processing resulted in overall lower A $\beta$  levels and a reduction in plaque burden. Here, we present for the first time clear in vivo evidence that global impairment of LRP1's endocytosis function favors non-amyloidogenic processing of APP due to its reduced internalization and subsequently, reduced amyloidogenic processing. By inactivation of LRP1, the inhibitory effect on A $\beta$  generation overrules the simultaneous impaired A $\beta$  clearance, resulting in less extracellular A $\beta$  and reduced plaque deposition in a mouse model of AD.

**Keywords** Alzheimer's disease · Animal model · APP · LRP1 · APP metabolism · A $\beta$  clearance

Bart Van Gool and Steffen E. Storck contributed equally to this work.

**Electronic supplementary material** The online version of this article (<https://doi.org/10.1007/s12035-019-1594-2>) contains supplementary material, which is available to authorized users.

✉ Anton J. M. Roebroek  
anton.roebroek@kuleuven.be

<sup>1</sup> Laboratory for Experimental Mouse Genetics, Department of Human Genetics, KU Leuven, Herestraat 49, Box 604, 3000 Leuven, Belgium

<sup>2</sup> Institute for Pathobiochemistry, University Medical Center, Johannes Gutenberg University of Mainz, Mainz, Germany

<sup>3</sup> Department of Medicine, Division of Endocrinology and Metabolism, University of California San Diego, La Jolla, CA 92093, USA

<sup>4</sup> SANOFI, Neuroscience Therapeutic Area, 1 Avenue P. Brossolette, 91385 Chilly-Mazarin, France

## Introduction

One of the hallmarks of Alzheimer's disease (AD) pathogenesis is the accumulation of amyloid- $\beta$  (A $\beta$ ) in the brain. It has been shown that this A $\beta$  accumulation is the result of a disturbed balance of A $\beta$  generation from its precursor APP and its subsequent clearance. In sporadic or the common late-onset AD, impaired clearance of A $\beta$  is apparently predominantly responsible for its accumulation rather than A $\beta$  overproduction [1]. To date, several mechanisms in the brain have been identified that are involved in the clearance of extracellular A $\beta$  from brain interstitial fluid (ISF) and cerebrospinal fluid (CSF). These include cellular uptake followed by intracellular degradation by neurons, microglia, pericytes and astrocytes, extracellular degradation by enzymes in the ISF, efflux into the periphery by blood-brain barrier (BBB) clearance, and ISF bulk-flow clearance to the CSF sink or perivascular spaces followed by degradation or drainage into the circulatory or lymphatic system ([2, 3], reviewed in [4]). The low-density lipoprotein receptor-related protein-1 (LRP1) plays a pivotal

role in A $\beta$  clearance (reviewed in [5]) by mediating receptor-mediated A $\beta$  uptake and degradation in astrocytes, neurons and cerebrovascular smooth muscle cells [6–8], or a concerted A $\beta$  transcytosis together with ABCB1/P-glycoprotein (P-gp) across the BBB [9–12]. In addition, cellular models have shown that LRP1 is also a modulator of APP processing driving A $\beta$  generation via interactions between the intracellular and extracellular domains of both transmembrane proteins LRP1 and APP [13–18]. These seemingly opposing roles of LRP1 on A $\beta$  metabolism have raised the question to what extent LRP1 expression affects A $\beta$  pathology in the brain.

APP is a single-pass transmembrane protein, and alternative splicing of the APP transcript generates many different isoforms of which three are most common: the 695 (APP<sub>695</sub>; predominantly expressed in CNS), the 751 (APP<sub>751</sub>), and 770 (APP<sub>770</sub>) amino acid forms [19]. APP isoforms encoding the Kunitz protease inhibitor domain in their extracellular part (i.e., APP<sub>751</sub> and APP<sub>770</sub>) interact directly via this domain with a ligand-binding domain in the extracellular part of LRP1 [13, 14]. The cytoplasmic FE65 adaptor protein on the other hand can form a functional link between the intracellular domains of APP and LRP1 [15]. These interactions between LRP1 and APP allow internalization of APP into the endosomal compartment. Depending upon relative expressions levels of LRP1, of the different APP isoforms and of other involved proteins like FE65, internalization of APP and subsequent generation of A $\beta$  can be modulated. Upon internalization of APP, amyloidogenic proteolytic cleavage by beta- and gamma-secretases results in the generation of A $\beta$  and a soluble APP- $\beta$  (sAPP- $\beta$ ) fragment. In contrast, non-amyloidogenic proteolytic cleavage of APP by alpha-secretase at the cell surface results in secretion of soluble APP- $\alpha$  (sAPP- $\alpha$ ) and precludes generation of the detrimental A $\beta$  peptide (reviewed in [5, 20]).

LRP1 is a single-pass transmembrane receptor that binds over 40 different ligands and is as endocytic and signaling receptor involved in many different physiological processes (reviewed in [5, 21]). After proteolytic cleavage of the LRP1 precursor, the mature LRP1 receptor consists of a large extracellular 515-kDa  $\alpha$ -subunit (LRP1- $\alpha$ ) non-covalently attached to its 85-kDa  $\beta$ -subunit (LRP1- $\beta$ ), consisting of an extracellular, a transmembrane, and an intracellular domain. This intracellular domain encodes many motifs, including the NPxY (xxL) motifs, interacting with adaptor and scaffold proteins. In comparison with the proximal NPxY and distal NPxY motif (within the NPxYxxL motif) and two di-leucine motifs, the YxxL motif (within the NPxYxxL motif) is apparently the predominant internalization motif in LRP1 [22]. Noteworthy is to mention that FE65 binds to the NPxYxxL motif to form a functional link between the intracellular domains of APP and LRP1, triggering the internalization of the complex and subsequent the generation of A $\beta$  [15]. DAB1, on the other hand, competes with FE65 for LRP1 binding, resulting in a reduction of amyloidogenic APP processing [23].

Previously, we reported on the generation of a series of LRP1 knock-in mice by recombinase-mediated cassette exchange [24, 25]. In these mice, the proximal NPxY motif (also indicated by NPxY1) and/or the distal NPxYxxL motif (here indicated by NPxY2) in the intracellular domain are inactivated. The rationale to generate these mouse models was to unravel the complex biological function of the receptor LRP1 by partial impairment of the function of the endogenous LRP1 receptor. Characterization of the knock-in mouse models revealed that combined inactivation of the NPxY1 and NPxY2 motifs results in embryonic lethality between E10.5 and E13.5 reminiscent of the full LRP1 knock-out [24]. Inactivation of just NPxY1 presents late fetal lethality due to the impaired early LRP1 biosynthesis, which results in low levels of mature LRP1 reaching the cell surface [24]. Inactivation of NPxY2 (simultaneous inactivation of the overlapping NPxY and YxxL motifs) was initially not linked to a clear phenotype [25], but in a LDLR-deficient mouse model, inactivation of NPxY2 enhances postprandial dyslipidemia and atherosclerosis demonstrating that NPxY2 is essential for the atheroprotective role of LRP1 [26]. Furthermore, NPxY2 inactivation was shown in vitro in mouse-derived cells to compromise LRP1 endocytosis rates of ApoE,  $\alpha_2$ M and NR2B NMDA receptor subtype, and  $\beta$ 1-integrin [24, 27–29]. This is mainly a consequence of inefficient slow recycling of the mutated receptor [27]. We also identified the NPxY2 motif of LRP1 as a crucial element for LRP1-NMDA receptor interaction via the adaptor protein PSD95 and relevant for tPA activation of the LRP1-NMDA receptor complex in derived neuronal cells [30]. Finally, inactivation of NPxY2 resulted in impairment of transcytosis of A $\beta$ 1–40 across a brain endothelial monolayer [10].

In the current study, we sought to study the dual role of LRP1 on A $\beta$  metabolism in vivo. We report on the in vivo impact of the LRP1-inactivating NPxY2 mutation on APP processing in a mouse model overexpressing human APP. Our results provide the first in vivo evidence that in accordance with the cellular in vitro models, endogenous LRP1 contributes to the generation of A $\beta$  and simultaneously is a receptor for A $\beta$  clearance. A loss of LRP1 function results in a reduction of A $\beta$  clearance, but at the same time favors non-amyloidogenic APP processing, reducing the overall generation of A $\beta$  and leading to a diminished A $\beta$  pathology in brain.

## Methods

### Mice

Generation of a LRP1-NPxY2 mutant knock-in mouse with inactivation of the membrane distal NPxY2 (NPVYATL  $\rightarrow$  AAVAATL) motif was already described in detail before [25]. For analysis of the in vivo effect of

inactivation of the membrane distal NPxY2 motif on the APP metabolism in a AD mouse model, LRP1-NP<sub>x</sub>Y2 mutant mice were crossed with the Thy1-hAPP<sub>751</sub>SL AD mouse model described by Blanchard et al. [31], overexpressing a human APP<sub>751</sub> isoform carrying the Swedish and London mutations. Breeding pairs of heterozygous LRP1-NP<sub>x</sub>Y2 mutant knock-in mice of which the male or female was additionally carrying the Thy1-hAPP<sub>751</sub>SL transgene were used to generate inbred LRP1 wildtype mice and homozygous LRP1-NP<sub>x</sub>Y2 mutant knock-in mice, without or hemizygous for the Thy1-hAPP<sub>751</sub>SL transgene (mixed C57Bl/6J and 129 background). Unless otherwise stated, female mice of an age of 9 months were analyzed in a comparative study. For in vitro endothelial transcytosis analysis, inducible brain endothelial-specific LRP1 knock-out mice (*Lrp1*<sub>BE</sub><sup>-/-</sup>) were used as described in detail before [12]. The research was approved by the Ethical Committees for Animal Experimentation of the KU Leuven and the Johannes Gutenberg University of Mainz and the ethical committee on animal care and use of Rhineland-Palatinate, Germany.

### Isolation of Total Protein Homogenates and Protein Fractionation from Mice Brains

Mice, euthanized by CO<sub>2</sub> intoxication or pentobarbital (100 mg/kg, i.p.), were perfused transcardially with PBS. After isolations of the brains, hemispheres were snap-frozen in liquid nitrogen and stored at -80 °C until further processing. For the analysis of APP metabolism in protein subfractions, 6-ml ice-cold buffer [20-mM Tris-HCl, 1× complete proteinase cocktail (Roche) (pH 8.5)] per gram frozen tissue was used for homogenization with a cooled glass-Teflon Potter-Elvehjem type of homogenizer (18 strokes, 350 rpm). Total protein homogenates were obtained after brief centrifugation (12,000 g, 15 min, 4 °C) to remove debris. Small aliquots of the total protein homogenates were stored at -20 °C, whereas the remaining large aliquots were used according to a differential extraction procedure to obtain fractions containing soluble proteins, TX100-soluble membrane proteins, and insoluble or “plaques”-associated proteins as described before with minor modifications [32]. After an initial centrifugation step (100,000 ×g for 80 min at 4 °C, Beckman TL100), the supernatant was collected as soluble protein fraction, whereas the pellet fraction was resuspended in 6-ml ice-cold buffer supplemented with 1% TX100 per gram pellet fraction. After a next centrifugation step (100,000 ×g for 80 min at 4 °C, Beckman TL100), the supernatant was collected as the TX100-soluble membrane protein fraction. All fractions were stored at -20 °C until analysis. For analysis of the different Aβ species in PBS-soluble protein fractions by a combination of immunoprecipitation and western blot analysis, a different fractionation protocol was used [12]. Briefly, brain hemispheres were homogenized in

1000-μL PBS containing complete protease and phosphatase inhibitor (Roche Applied Science) using a glass homogenizer (30 strokes) and subsequently centrifuged at 55,000 g for 20 min at 4 °C. The supernatant containing secreted PBS-soluble brain Aβ was collected and stored at -20 °C for further analysis.

### Western Blot Analysis of APP and APP Metabolites and ELISA for Aβ

Protein concentrations of the soluble protein fractions and of the TX100-soluble membrane protein fractions were determined by the bicinchoninic acid assay kit (PIERCE, Perbio, France), and samples containing 10-μg protein were prepared in LDS sample buffer (Invitrogen NP-009). After reduction and denaturation at 95 °C for 10 min, the samples were loaded and separated by PAGE on 4–20% or 10% Tris-glycine (Anamed, Germany) and transferred onto nitrocellulose membranes. Ponceau S (Sigma-Aldrich) was used to confirm loading of equal amounts of protein and to monitor the transfer procedure. After blocking with blocking buffer [TBS (50-mM Tris, 150-mM NaCl, pH 7.6) containing 0.1% Tween 20 and 5% milk], the membranes were probed overnight (4 °C) with a primary antibody diluted in blocking buffer. Membranes were rinsed in TBS containing 0.1% Tween 20 and incubated with appropriate horseradish peroxidase (HRP)-conjugated secondary antibodies diluted in blocking buffer. Careful execution of the homogenization and fractionation procedures in combination with the Ponceau S staining of the blots confirmed loading and subsequent transfer of equal amounts of protein in the analyzed protein fractions (see Supplementary Fig. 1a, Supplementary Fig. 2a, b). In the case of western blot analysis of total homogenates, usually, normalization of western blot expression levels to housekeeping genes, like actin or tubulin, is done. At first sight, use of analysis of actin expression in combination with a fractionation procedure following upon homogenization appears less suitable, but in our fractionation procedure the distribution of actin between the soluble protein fraction and TX100-soluble membrane protein fractions was shown to occur according a relatively stable and reproducible ratio (see Supplementary Fig. 1b), confirming also in this way loading and transfer of equal amount of protein in the analyzed protein fractions. Moreover, we analyzed up to *n* = 5–6 animals per group to get representative results.

For detection of immature and mature APP in the TX100-soluble membrane protein fraction, the primary rabbit polyclonal antibody B10.4 (homemade, directed against the 20 carboxy-terminal amino acids of APP) was used. For detection of total sAPP and sAPP-α in the soluble protein fraction, the primary mouse monoclonal antibodies 22C11 (Chemicon, directed against aa 6–81 of APP) and 6E10 (Chemicon, directed against aa 1–17 of Aβ) were used respectively. For detection of

sAPP- $\beta$  in the soluble protein fraction, a rabbit antibody (Signet, 9138-005) was used. Mouse anti-tubulin (T8328, Sigma-Aldrich), mouse anti-synaptophysin (101011, Synaptic Systems), and mouse anti-PSD-95 (P43520, BD Transduction Laboratories) were used to control for equal loading of membrane fractions. Finally, mouse monoclonal anti- $\beta$ -actin clone AC-15 (Sigma-Aldrich) was used for analysis of actin expression. Secondary antibodies were conjugated with HRP. Western blots were developed by chemiluminescence (Western Lightning ECL Pro; Perkin-Elmer) followed by digital picture acquisition and analysis (LAS 4000; ImageQuant v7.0; GE Healthcare). Final blot pictures were equally adjusted to enhance visibility using Adobe Photoshop (version 7.0) (Adobe Systems, San Jose, USA).

### Immunoprecipitation of Total A $\beta$ from PBS-Soluble Protein Fractions and Subsequent A $\beta$ Separation with 8-M Urea SDS Gel and Western Blotting

Total A $\beta$  was immunoprecipitated from 1000- $\mu$ g protein of PBS-soluble protein fractions by mixing fivefold concentrated detergent buffer [50-mM HEPES (pH 7.4), 150-mM NaCl, 0.5% (v/v) Nonidet P-40, 0.05% (w/v) SDS, and protease inhibitor cocktail (Roche Applied Science)] with the respective samples. Magnetic Dynabeads (M-280 Sheep Anti-Mouse IgG, 11201D, Novex) containing sheep anti-mouse IgG attached to their surface were precoated with IC16 antibody directed against the first 16 amino acids of A $\beta$  [33] according to the manufacturer's protocols, and equal amounts of IC16 antibody-covered beads were added to the samples as shown by the immunoreactivity of IC16 light chain displayed in Supplementary Fig. 3. After overnight incubation at 4 °C, samples were washed 3 times in PBS, 0.1% (w/v) BSA, and once in 10-mM Tris-HCl, pH 7.5. After heating the samples to 95 °C in 25- $\mu$ l sample buffer [0.36-M Bis-Tris, 0.16-M bicine, 1% (w/v) SDS, 15% (w/v) sucrose, and 0.0075% (w/v) bromphenol blue], the supernatants were subjected to PAGE. Separation of immunoprecipitated A $\beta$  peptides was performed on 0.75-mm 10% T/5% C polyacrylamide 8-M urea SDS gels. For separation of A $\beta$ 1–40 from A $\beta$ 1–42, a final concentration of 0.3-M H<sub>2</sub>SO<sub>4</sub> was used in resolving gels. This has the effect that peptides are separated not only according to their molecular weight but also according to their hydrophobicity and results that A $\beta$ 1–42 migrates faster than A $\beta$ 1–40. Peptides were transferred to an Immobilon-P PVDF membrane via semi-dry western blotting (Bio-Rad) at 46 mA for 45 min. Membranes were boiled for 3 min in PBS and blocked in 5% skim milk in TBST [20-mM Tris, 137-mM NaCl, 0.1% (v/v) Tween-20] for 30 min afterward. A $\beta$  peptides were detected with IC16 antibody and donkey anti-mouse second antibody conjugated with HRP using enhanced chemiluminescence (Millipore, Schwalbach, Germany) and

digital picture acquisition (LAS-3000mini, Fujifilm, Duesseldorf, Germany).

### Isolation of Cerebrospinal Fluid for A $\beta$ ELISA

For isolation of CSF from the cisterna magna, the method previously described by DeMattos was used [34]. Subsequently, the A $\beta$ 40 and A $\beta$ 42 levels in the CSF were determined by A $\beta$ 40 and A $\beta$ 42 specific ELISA kits, according to the manufacturer's instructions (the Genetics Company).

### Isolation and Culture of Primary Mouse Brain Capillary Endothelial Cells

Primary mouse brain capillary endothelial cells were isolated from 12- to 15-week-old mice according to a standard protocol as described previously [10, 35]. Cells were plated on 24-well Transwell filters (pore size, 0.4  $\mu$ m; surface area, 33.6 mm<sup>2</sup>; Greiner Bio-One) coated with collagen IV/fibronectin (Sigma-Aldrich). Cultures were maintained in DMEM supplemented with 20% plasma-derived bovine serum (First Link), 100-U/ml penicillin (Gibco), 100- $\mu$ g/ml streptomycin (Gibco), 2-mM L-glutamine (Gibco), 4- $\mu$ g/ml puromycin (Alexis), and endothelial cell growth supplement (E2759, Sigma) at 37 °C and 5% CO<sub>2</sub>. Cells were cultured in the cellZscope device, in which transendothelial electrical resistance (TEER) and capacitance were monitored over time. Puromycin was withdrawn after 4 days in culture. When cells reached confluency and the capacitance was around 1  $\mu$ F/cm<sup>2</sup>, culture medium was removed, and serum-free DMEM/Ham's F12 (Gibco) medium containing 1-mM L-glutamine, 100-U/ml penicillin, and 100- $\mu$ g/ml streptomycin was added. Five hundred fifty nM hydrocortisone (Sigma-Aldrich) was supplemented to induce high TEER. The following day transport studies were performed.

### In Vitro Transcytosis of [<sup>125</sup>I]-A $\beta$ 1–42

In order to study A $\beta$  transcytosis in vitro, a standard transport model was used [10, 12, 35]. [<sup>125</sup>I]-A $\beta$ 1–42 (0.1 nM) (purchased from Phoenix Peptide) and 1- $\mu$ Ci/ml [<sup>14</sup>C] inulin (purchased from PerkinElmer), a marker for paracellular diffusion, were added to serum-free media supplemented with 550-nM hydrocortisone and 40-mM HEPES and incubated at 37 °C. To study brain-to-blood transport, 10- and 80- $\mu$ l samples were taken from the luminal compartment 60 min after the addition of [<sup>125</sup>I]-A $\beta$ 1–42 and [<sup>14</sup>C]-inulin to the abluminal compartment. To investigate the amount of intact [<sup>125</sup>I]-A $\beta$ 1–42 transported to the luminal side, 80- $\mu$ l 15% TCA was added to an 80- $\mu$ l luminal media sample and incubated for 10 min at 4 °C. Samples were then centrifuged at 16,000 g for 10 min. Pellets (representing intact [<sup>125</sup>I]-A $\beta$ 1–42) were counted for



[ $^{125}\text{I}$ ]. Probes were counted on a Wallac Wizard2 2470 automatic  $\gamma$ -counter (PerkinElmer) for [ $^{125}\text{I}$ ] or on a Tri-Carb 2800 TR Liquid Scintillation Analyzer (PerkinElmer) for [ $^{14}\text{C}$ ]. Transport of intact [ $^{125}\text{I}$ ]-A $\beta$ 1–42 across the monolayer was calculated as A $\beta$ 1–42 transcytosis quotient (TQ) using the following formula:

$$\text{A}\beta 1-42 \text{ TQ} = ([^{125}\text{I}]\text{-A}\beta 1-42 \text{ luminal} / [^{125}\text{I}]\text{-A}\beta 1-42 \text{ input}) / ([^{14}\text{C}]\text{-inulin acceptor} / [^{14}\text{C}]\text{-inulin input})$$

### Brain Clearance of [ $^{125}\text{I}$ ]-A $\beta$ 1–42

To measure the brain clearance of [ $^{125}\text{I}$ ]-A $\beta$ 1–42, we used a similar method as described previously [12]. 0.5- $\mu\text{l}$  tracer fluid containing 1  $\mu\text{Ci}/\text{ml}$  [ $^{14}\text{C}$ ]-inulin (reference marker) and pathophysiological amounts of [ $^{125}\text{I}$ ]-A $\beta$ 1–42 (5.14 nM) was injected with a 26-gauge needle attached to an UltraMicroPump controller (UMP3-1, Word Precision Instruments) over 5 min into ISF of the right caudate putamen (0.9 mm anterior from bregma, 1.9 mm lateral from midline, and 2.9 mm below the surface) of 4 months old and sex-matched mice anesthetized with ketamine (800 mg/kg) and medetomidine (5 mg/kg). After injection, the microsyringe was left in place for 5 min. Blinded brain samples were collected at 10 min after injection and prepared for analysis. In vivo [ $^{125}\text{I}$ ]-A $\beta$ 1–42 clearance was calculated as follows: 100% recovery in brain after 15 min. The percentage of radioactivity remaining in the brain was calculated as follows: % recovery in brain =  $100 \times (N_b / N_i)$ , where  $N_b$  is the radioactivity in the brain at the end of the experiment and  $N_i$  is the radioactivity injected into the brain, as illustrated by TCA-precipitable [ $^{125}\text{I}$ ]-radioactivity (measured in cpm).

### Immunohistochemistry

Mice, euthanized by  $\text{CO}_2$  intoxication, were perfused transcardially with PBS followed by a 4% paraformaldehyde (PFH) solution in phosphate-buffered saline (PBS). After isolation of the brains, brains were postfixated overnight in 4% PFH in PBS and finally rinsed in PBS. The brains were then dehydrated and embedded in paraffin for sectioning (7  $\mu\text{m}$  in thickness). Paraffin-embedded brain sections were dewaxed and rehydrated, the epitope was exposed in 1/3 formic acid for 7 min, and endogenous peroxidase was quenched with hydrogen peroxide [3% (v/v) in methanol] for 10 min. After sufficient washing with PBS, slides were incubated for 5 min in PBS supplemented with 1% Tween 20 followed by 2 h in a blocking buffer [5% goat normal serum, 2% BSA, 0.5% blocking reagent (Perkin Elmer), 10-mM Tris-HCl, 150-mM NaCl, pH 7.5]. The primary antibody diluted in blocking buffer was applied overnight at 4  $^\circ\text{C}$ . Following sufficient

washing, secondary antibody diluted in blocking buffer was applied for 2 h at RT. For analysis of the plaque load, primary mouse monoclonal antibody 6E10 (Chemicon, directed against amino acids 1–17 of A $\beta$ ) and secondary antibody GAM-HRP were used, and the signal was visualized with the TSA<sup>TM</sup> PLUS kit from Perkin Elmer according to the manufacturer's instructions. Photographs were taken with a Leica MZ FLIII stereomicroscope. The number of plaques and the percentage of the brain covered with plaques was analyzed by ImageJ 1.41 software from the National Institute of Health (NIH) on four consecutive sections from each mouse around bregma  $-2.5$ .

### Statistical Analysis

Statistical significance was assessed using Student's *t* test. Whenever necessary, data were logarithmically transformed to meet *t* test assumptions.  $p < 0.05$  was regarded statistically significant.

## Results

### Decreased Brain Clearance of A $\beta$ in Mice Carrying the NPxY2 Knock-in Mutation

Previously, we have shown that primary endothelial cells derived from LRP1<sup>NPxY2/NPxY2</sup> mice show reduced transport of A $\beta$  across the endothelial cells compared with those from LRP1<sup>WT/WT</sup> mice, corroborating that LRP1 is an important clearance receptor for neurotoxic A $\beta$  from brain [9, 10]. In our present analysis, we verified our original findings (Fig. 1a, b), showing that transcytosis of A $\beta$ 1–42 was reduced in endothelial cells carrying the LRP1 NPxY2 knock-in mutation compared to wild-type (wt) endothelial cells. The reduction in transport we observed was comparable to endothelial cells deficient of LRP1 (KO) implicating that A $\beta$  transport capacity is highly impaired by the NPxY2 knock-in mutation [12]. These data again demonstrated that on a cellular level, impaired LRP1 function due to its decreased internalization leads to decreased A $\beta$  clearance. LRP1 expression is not restricted to cells compromising the BBB. In fact, it has been shown that also neuronal, astrocytic LRP1, and also LRP1 in smooth muscle cells contribute to the clearance of A $\beta$  in vivo [6, 7, 36]. In order to study total brain clearance in vivo, we injected radiolabelled [ $^{125}\text{I}$ ]-A $\beta$ 1–42 into the caudate putamen of LRP1<sup>NPxY2/NPxY2</sup> and LRP1<sup>WT/WT</sup> mice (Fig. 1c). Whereas A $\beta$  was rapidly cleared from brain in LRP1<sup>WT/WT</sup> mice, LRP1<sup>NPxY2/NPxY2</sup> showed a significant impairment in A $\beta$  clearance from brain (Fig. 1d). Together, these results demonstrated that not only on a cellular level but also in vivo LRP1<sup>NPxY2/NPxY2</sup> mice show a reduction in the capacity of A $\beta$  clearance.

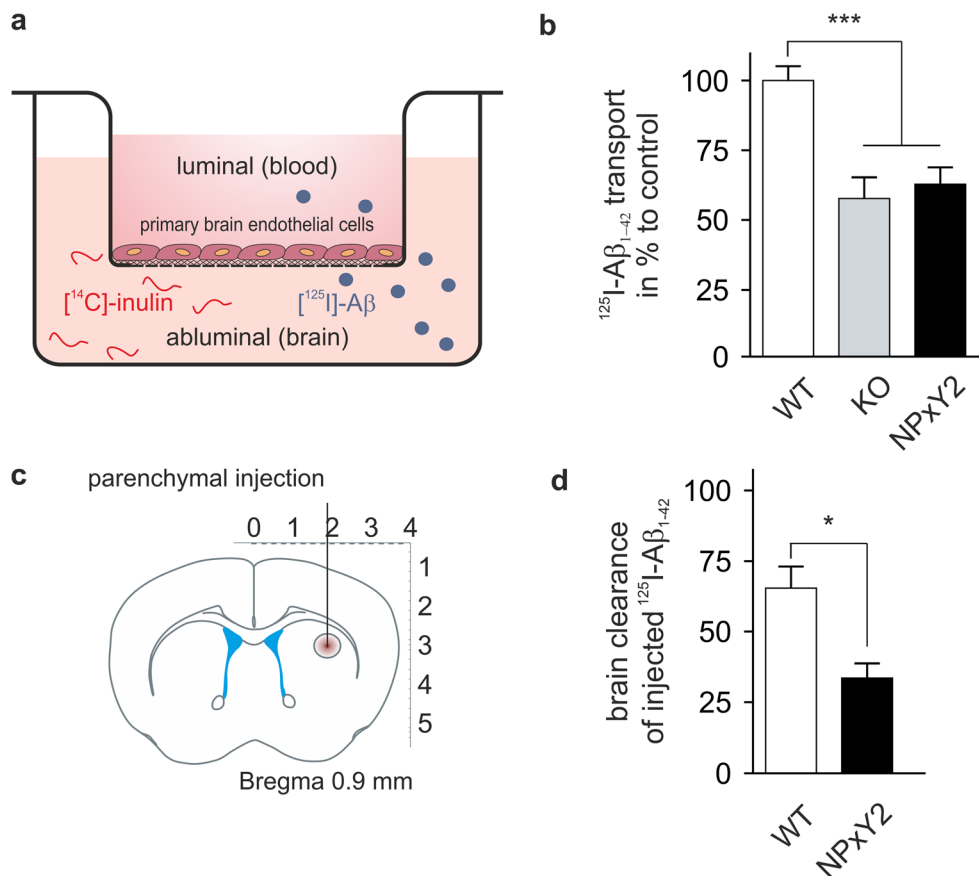


**Fig. 1** Decreased Aβ brain clearance and endothelial transcytosis in LRP1 NPxY2 mice. **a** Diagram illustrating the experimental procedure of [<sup>125</sup>I]-Aβ<sub>1-42</sub> transport across the primary mouse brain capillary endothelial cell monolayer cultured on Transwell inserts. **b** [<sup>125</sup>I]-Aβ<sub>1-42</sub> transport across the primary mouse brain capillary endothelial cell monolayer derived from control LRP1<sup>WT/WT</sup> (WT), LRP1<sup>BE-/-</sup> (brain endothelial-specific knock-out, KO), and LRP1<sup>NPxY2/NPxY2</sup> (NPxY2) mice was studied in the presence of 1-μCi/ml [<sup>14</sup>C]-inulin to determine the transcytosis quotient (TQ). Transcytosis was analyzed in the brain-to-blood direction (abluminal to luminal) by measuring the dpm for [<sup>14</sup>C]-inulin and the cpm for the TCA-precipitable [<sup>125</sup>I] radioactivity. Data of three independent experiments, *n* = 22 (WT), *n* = 12 (KO), and *n* = 17

(NPxY2) (age 12–15 weeks). **c** Diagram illustrating the experimental procedure of in vivo brain clearance in mice. **d** LRP1 NPxY2 knock-in mutation inhibits Aβ brain clearance in vivo in LRP1<sup>NPxY2/NPxY2</sup> (NPxY2) mice compared with control LRP1<sup>WT/WT</sup> (WT) mice. 5.14-nM [<sup>125</sup>I]-Aβ<sub>1-42</sub> was microinfused into brain ISF of the caudate nucleus. Efflux was studied 15 min after injection by determining remaining radioactivity in the brain. *n* = 4 (WT and NPxY2, age 4 months). Error bars represent SEM. For statistical analyses of the data in **b**, the following test was used: repeated-measures ANOVA followed by Bonferroni multiple comparisons. For statistical analyses of the data in **d**, Student's *t* test was used. \* indicates *p* < 0.05, \*\*\* indicates *p* < 0.001

As we saw that NPxY2-mutated LRP1 showed a reduction in Aβ clearance in vitro and in vivo, we crossed LRP1<sup>NPxY2/NPxY2</sup> mice with Thy1-hAPP<sub>751</sub>SL mouse model that expresses human APP bearing both the Swedish (K670N/M671L) and the London (V717I) mutations (LRP1<sup>NPxY2/hAPP<sub>751</sub>SL</sup>). We analyzed the CSF of 9-month-old mice by Aβ ELISA measures. Interestingly, we found that CSF concentrations of both Aβ<sub>40</sub> and Aβ<sub>42</sub> in LRP1<sup>NPxY2/hAPP<sub>751</sub>SL</sup> were significantly lower than in LRP1<sup>WT/hAPP<sub>751</sub>SL</sup> control mice (Fig. 2a). This finding seemed to contradict our original idea that Aβ should accumulate due to impaired brain clearance. Moreover, we analyzed the soluble levels of Aβ in the brain by homogenizing the brain hemispheres in PBS followed by immunoprecipitation. Corresponding to what we saw in the CSF, we found

significantly lower Aβ<sub>1-40</sub> and Aβ<sub>1-42</sub> levels in the PBS-soluble fraction of the brain as analyzed by SDS-urea gel electrophoresis (Fig. 2b). Although several measures showed lower Aβ levels in fluids of the CNS in mice with impaired LRP1 function, it seemed to contradict all findings from previous studies showing that LRP1 impairment results in the accumulation of Aβ due to impaired clearance [11, 12, 37].

Next, we analyzed APP expression in brains of LRP1<sup>NPxY2/NPxY2</sup>/hAPP<sub>751</sub>SL and LRP1<sup>WT/WT</sup>/hAPP<sub>751</sub>SL controls with western blot analysis after protein fractionation. Loading and subsequent transfer of equal amounts of protein in the analyzed protein fractions were confirmed by Ponceau S staining and analysis of the expression of actin, which was apparently distributed according to a reproducible and stable ratio between the soluble protein fractions and TX100-soluble

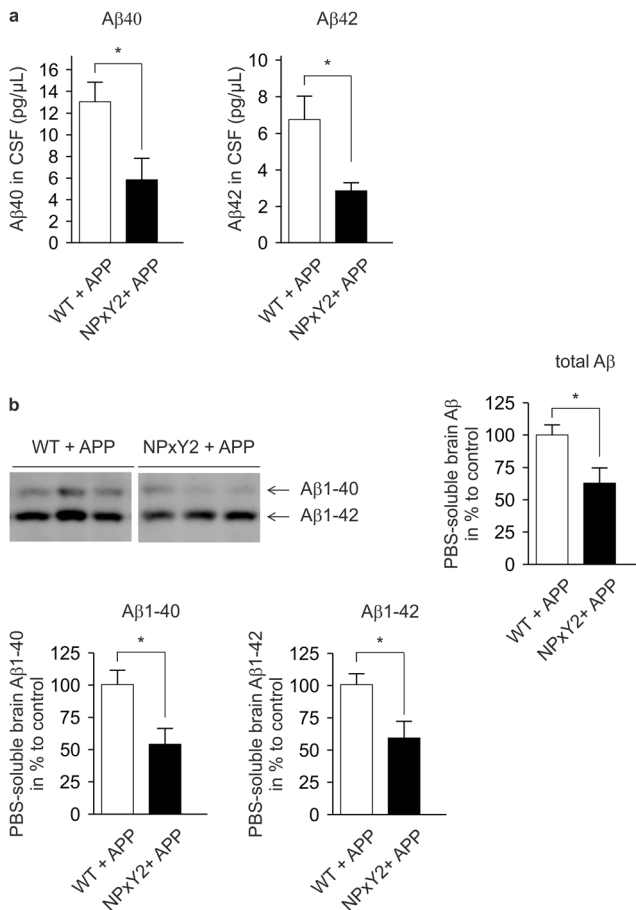


**Fig. 2** Decreased levels of Aβ in brain fluids of LRP1 NPxY2 mice. **a** ELISA on CSF obtained from the cisterna magna showed significant reduced levels for Aβ40 and Aβ42 in LRP1<sup>NPxY2/NPxY2</sup>/hAPP<sub>751</sub>SL (NPxY2 + APP) mice compared with LRP1<sup>WT/WT</sup>/hAPP<sub>751</sub>SL (WT + APP) mice. *n* = 10 for both groups (age 9 months). **b** WB analysis of the PBS-soluble protein fractions showed significant reductions in total Aβ, Aβ1–42, and Aβ1–40 levels in the NPxY2 + APP mice compared to control WT + APP. *n* = 5 (WT + APP) and *n* = 6 (NPxY2 + APP) (age 9 months). Error bars represent SEM, and statistical analysis was performed with Student's *t* test, \* indicates *p* < 0.05

membrane protein fractions (see Supplementary Fig. 1a, b). Additionally, we analyzed membrane proteins PSD-95 and synaptophysin as an internal control for equal loading of membrane fractions (see Supplementary Fig. 2a, b). We could not see any effects on the total mature and immature forms of APP in the TX100-soluble membrane protein fraction (Fig. 3a), indicating that no differences in APP expression are the reason for the reduced levels of Aβ found in CSF and PBS-soluble fractions. Analysis of the soluble protein fraction, however, showed that of LRP1<sup>NPxY2/NPxY2</sup>/hAPP<sub>751</sub>SL exhibited in significant increase of total sAPP and sAPP-α levels (Fig. 3b), suggesting that APP processing is altered in these mice. Vice versa, we could detect a trend towards lower sAPP-β levels that did not reach statistical significance (Fig. 3b).

The evident increase in sAPP-α and reduction in soluble total Aβ indicated that inactivation of LRP1 through its NPxY2 knock-in mutation shifts APP from amyloidogenic by beta-secretase to non-amyloidogenic processing by alpha-secretase at the cell surface, presumably due to impaired APP endocytosis by LRP1.

### Inactivation of the NPxY2 Motif Is Associated with a Reduced Aβ Plaque Load in Brains of APP<sub>751</sub>SL Mice

As our findings suggested that reduced endocytosis of APP by the impaired function of LRP1 promotes APP processing by alpha-secretase and thus lowering the generation of Aβ, we analyzed the plaque deposition in aged mice overexpressing human APP (hAPP<sub>751</sub>SL). Female mice were used, because they show an earlier phenotype than males.

Brain sections of 9-month-old female LRP1<sup>WT/WT</sup>/hAPP<sub>751</sub>SL and LRP1<sup>NPxY2/NPxY2</sup>/hAPP<sub>751</sub>SL mice were immunostained for Aβ (6E10 antibody) to visualize plaques. Analyses of four consecutive brain slices confirmed that the total number of plaques in the brain (Fig. 4a, b) as well as the percentage of the brain covered with plaques (Fig. 4a, c) was significantly reduced by 36 and 38% in the LRP1<sup>NPxY2/NPxY2</sup>/hAPP<sub>751</sub>SL mice when compared with the LRP1<sup>WT/WT</sup>/hAPP<sub>751</sub>SL controls. Therefore, inactivation of LRP1 does not only affect the soluble brain levels of Aβ but also influence its plaque deposition despite impaired Aβ clearance of LRP1.

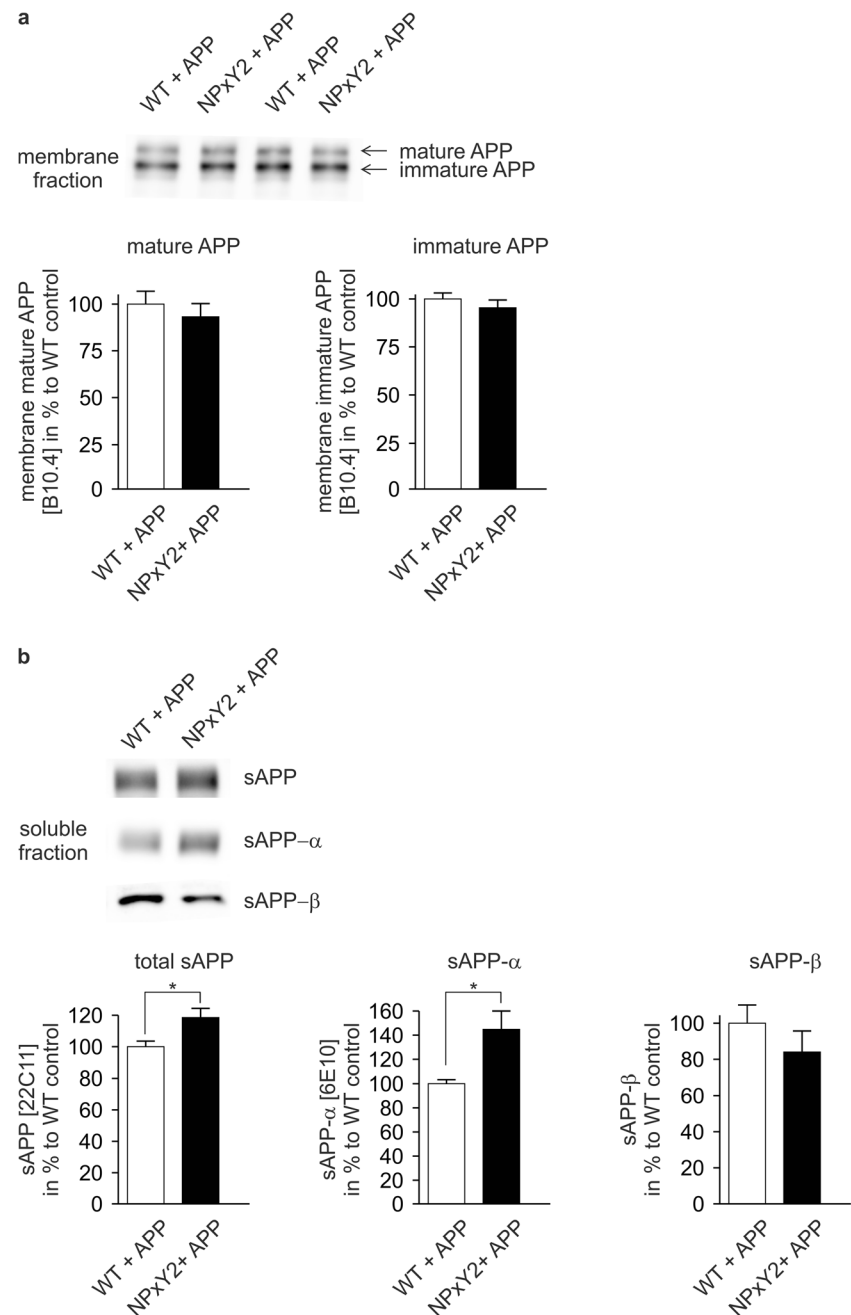
### Discussion

The objective of the present study was to investigate in vivo the impact of impaired LRP1 function on the APP processing. Previously, it has been shown that inactivation of the NPxY2 motif of endogenous LRP1 results in a partial inhibition of the endocytosis (and transcytosis in brain endothelial cells) of ligands or complexes with co-receptors by this LRP1 receptor [10, 24, 26–30]. In the present study, we could confirm that impairment of LRP1 endocytosis inhibits the brain clearance of Aβ in vitro and in vivo. At the same time, we found that impairment of LRP1 endocytosis influences the overall generation of Aβ by promoting alpha-secretase cleavage at the cell surface (as seen by higher sAPP-α levels) and the prevention of Aβ generation after endocytosis in vivo. Interestingly, our collective results suggest that despite impaired Aβ brain clearance due to the inactivation of LRP1, there is less accumulation of Aβ in CSF, ISF, and in plaques in a mouse model of AD in vivo.

This study clearly demonstrates that LRP1 has a dual role APP metabolism affecting both generation and clearance of Aβ. Many studies have shown both in vitro and



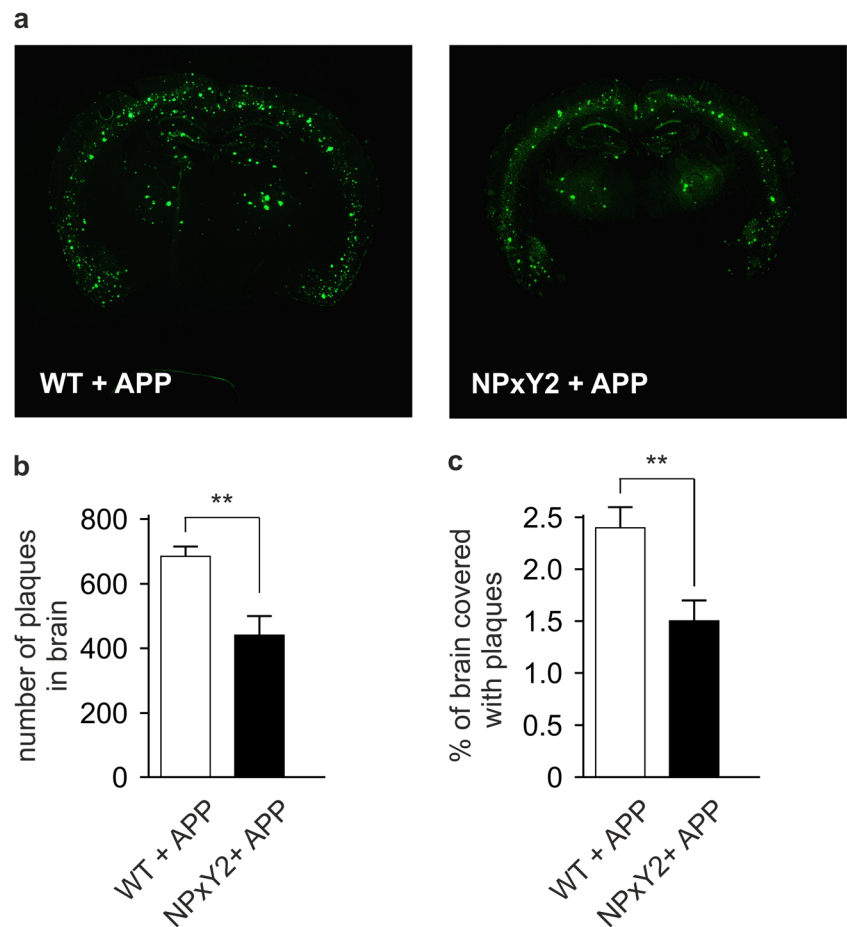
**Fig. 3** No difference in APP expression but difference in sAPP shedding in LRP1 NPxY2 knock-in mice. **a** WB analysis of the TX100-soluble membrane protein fractions showed no differences in the expression levels of unprocessed full length immature and mature APP in brains of LRP1<sup>NPxY2/NPxY2</sup>/hAPP<sub>751</sub>SL (NPxY2 + APP) mice compared with control LRP1<sup>WT/WT</sup>/hAPP<sub>751</sub>SL (WT + APP) mice. **b** WB analysis of the soluble protein fractions revealed a significant increase of total sAPP and sAPP- $\alpha$  in LRP1<sup>NPxY2/NPxY2</sup>/hAPP<sub>751</sub>SL (NPxY2 + APP) mice compared with control LRP1<sup>WT/WT</sup>/hAPP<sub>751</sub>SL (WT + APP) mice. The trend in reduction in sAPP- $\beta$  did not reach statistical significance. Number of mice analyzed:  $n = 6$  mice (WT + APP) and 5–6 (NPxY2 + APP) (age 9 months). Error bars represent SEM, and statistical analysis was performed with Student's  $t$  test, \* indicates  $p < 0.05$



in vivo that LRP1 is an important mediator in the clearance of A $\beta$  from the brain, e.g., in receptor-mediated endocytosis in astrocytes, neurons, and cerebrovascular smooth muscle cells [6–8]; in transcytosis across the BBB [9–12]. Cell type-specific deletion of LRP1 in astrocytes, neurons, smooth muscle cells, and endothelial cells has all led to a general increase of brain A $\beta$ . Studies on the general impact of LRP1 in different cell types on A $\beta$  metabolism or its effect on APP processing, and thus, the generation of A $\beta$  in vivo is scarce. Many in vitro studies support a role for LRP1 in the generation of A $\beta$  [13–18].

However, direct in vivo support for the involvement of LRP1 is limited. It has been shown that overexpression of a functional LRP1 mini-receptor in an APP transgenic mouse model [38] resulted in an age-dependent increase of soluble brain A $\beta$  [39]. These observations in this overexpressing mouse model support our findings and LRP1's role in amyloidogenic processing of APP in vivo. This study, for the first time, has modulated endogenous and global LRP1 function and has studied the effect on A $\beta$  metabolism. Overall inhibition of endogenous LRP1 is expected to simultaneously affect generation and

**Fig. 4** Plaque load in brain is significantly reduced in LRP1 NPxY2 mice. **a** Brain slices (bregma  $-2.5$ ) of LRP1<sup>WT/WT</sup>/hAPP<sub>751</sub>SL (WT + APP) and LRP1<sup>NPxY2/NPxY2</sup>/hAPP<sub>751</sub>SL (NPxY2 + APP) mice were immunostained with the antibody 6E10, and plaques were visualized with the TSA<sup>TM</sup>PLUS kit from Perkin Elmer. Pictures show representative stainings for WT + APP and NPxY2 + APP mice. **b** The number of plaques as determined in 6E10-immunostained brain slices via ImageJ software from NIH. **c** The percentage of the brain covered with plaques as determined in 6E10-immunostained brain slices via ImageJ software from NIH. For **b** and **c**,  $n = 10$  for LRP1<sup>WT/WT</sup>/hAPP<sub>751</sub>SL (WT + APP) mice and  $n = 8$  for LRP1<sup>NPxY2/NPxY2</sup>/hAPP<sub>751</sub>SL (NPxY2 + APP) mice (age 9 months). Error bars represent SEM, and statistical analysis was performed with Student's *t* test, \* indicates  $p < 0.05$



clearance of A $\beta$ , in which opposing effects could mask each other. In our present study, we see both: due to LRP1 inactivation in vivo brain clearance and, at the same time, the generation of A $\beta$  is impaired. Still, the net effect of impaired LRP1 function on brain A $\beta$ , despite its impaired clearance, is a lesser accumulation of A $\beta$  in the brain.

Thus, the present results are a direct in vivo support that LRP1 is involved in amyloidogenic APP processing. Hence, the receptor that is involved in the generation of potentially toxic A $\beta$  through receptor-mediated endocytosis of APP, at the same time, keeps soluble brain A $\beta$  low by the constant clearance of A $\beta$  from ISF and CSF through endocytosis and subsequent degradation or transcytosis across the BBB (see Fig. 5). The clearance function of LRP1 in the different cells of the brain seems crucial as multiple cell-specific knock-out mouse models have shown that LRP1 ablation leads to a net accumulation of A $\beta$  in the brain. One has to say that this carefully balanced system of A $\beta$  production and clearance is influenced not only by LRP1 expression itself but also by other members of the LDLR family that modulate APP endocytosis (reviewed in [40]). Therefore, changes in expression of different LDLR family members will modulate the generation versus clearance machinery. However, our study concentrating on LRP1 function on APP metabolism in vivo suggests that LRP1 is actually promoting the generation

of A $\beta$ , while at the same time preventing its accumulation by mediating its clearance.

It is noteworthy to say that it is most likely not feasible to target LRP1 expression in the brain to reduce the production of A $\beta$ : LRP1 has numerous other functions besides mediating endocytosis. Over the years, studies have shown that LRP1 is involved in many important cellular processes, including cell signaling, cell migration, proliferation, angiogenesis, and wnt signaling modulation ([41], reviewed in [42]). Embryonic lethality of global LRP1 knock-out mice shows the importance of the receptor in these processes during development. On the other hand, cell-specific LRP1 knock-out mouse models have shown that clearance of A $\beta$  can be modulated by LRP1 expression [6, 7, 12, 36]. As it is unlikely that we can control LRP1-mediated production of A $\beta$ , future therapeutic approaches should concentrate on enhancing LRP1-mediated A $\beta$  clearance from the brain.

In conclusion, our findings for the first time show that endogenous LRP1 has a predominate role in regulating the processing of APP in vivo. Our analysis in a mouse model of AD shows that impairment of LRP1 inhibits A $\beta$  brain clearance but simultaneously reduces its production resulting in an overall reduced A $\beta$  pathology in the brain and therefore gives important insights in the molecular mechanisms underlying metabolism of A $\beta$  in vivo.

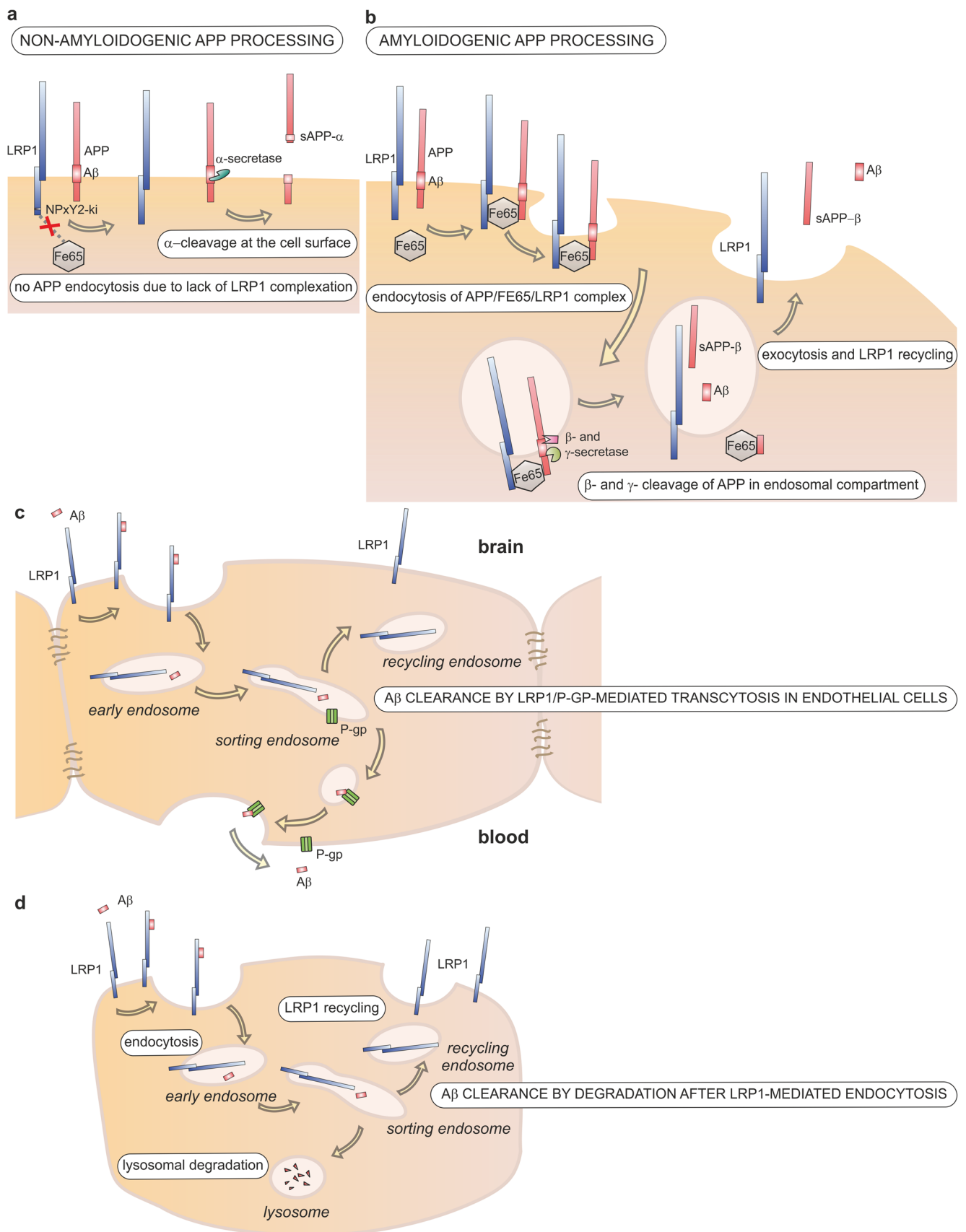


**Fig. 5** The role of LRP1 in APP processing and A $\beta$  clearance in the brain. **a** Schematic representation of non-amyloidogenic processing of APP:  $\alpha$ -cleavage at the cell surface by  $\alpha$ -secretase precludes generation of A $\beta$  and results in generation of sAPP- $\alpha$ . The lack of FE65 binding to the LRP1 NPxY2 domain due to the knock-in mutation reduces APP internalization. **b** Schematic representation of amyloidogenic processing of APP: LRP1 mediates the internalization of the APP/LRP1/FE65 complex, which results in the intracellular generation of A $\beta$ . Interaction between FE65 and the intracellular domains of APP and LRP1 triggers the internalization of the tripartite complex. Subsequent  $\beta$ - and  $\gamma$ -cleavage by  $\beta$ - and  $\gamma$ -secretases in the endosomal compartment results in the generation of A $\beta$  and sAPP- $\beta$ , which are both secreted by exocytosis, a process that simultaneously results in the recycling of LRP1 to the cell surface. **c** Involvement of LRP1 A $\beta$  clearance from brain ISF in the brain by endothelial transcytosis across the blood-brain barrier. In ISF-circulating A $\beta$  is internalized by LRP1 and handed over to ABCB1/P-glycoprotein (P-gp) probably in the sorting endosome. P-gp exocytoses A $\beta$  at the luminal side of the endothelium, whereas LRP1 is recycled to the cell surface. **d** Endocytosis by astrocytes, neurons, smooth muscle cells, and other cells in the brain results in lysosomal degradation of A $\beta$

**Acknowledgements** We thank SANOFI for the use of their AD mouse model in this study. We thank Leen Verbeek for technical assistance.

**Funding Information** This work was supported by grants from the American Health Assistance Foundation (Alzheimer's Disease Research, A2007-096) and the Belgian SAO-FRMA (Foundation Alzheimer Research, grants ISAO 04602 and SAO-FRMA 06601) to AR. The research was also funded by a PhD grant of the Institute for Innovation through Science and Technology in Flanders (IWT-Vlaanderen) to SR. The project was funded by grants of the Deutsche Forschungsgemeinschaft (PA930/12, PI 379/8-1) and JPND joint EU grant (PROP-AD: BMBF #01ED1605—Germany) to CP and the intramural funding program of the University Medical Center of the Johannes-Gutenberg University Mainz to SS.

## Compliance with Ethical Standards

**Conflicts of Interests** The authors declare that they have no conflicts of interests. LP is a full employee of SANOFI, a pharmaceutical company, but he declares that he has no conflict of interest with regard to the present study.

**Research Involving Human Participants and/or Animals** This article does not contain any studies with human participants performed by any of the authors.

**Ethical Approval** The research was approved by the Ethical Committees for Animal Experimentation of the KU Leuven and the Johannes Gutenberg University of Mainz and the ethical committee on animal care and use of Rhineland-Palatinate, Germany. All applicable international, national, and/or institutional guidelines for the care and use of animals were followed. All procedures performed in studies involving animals were in accordance with the ethical standards of the institutions or practice at which the studies were conducted.

**Open Access** This article is distributed under the terms of the Creative Commons Attribution 4.0 International License (<http://creativecommons.org/licenses/by/4.0/>), which permits unrestricted use, distribution, and reproduction in any medium, provided you give appropriate credit to the original author(s) and the source, provide a link to the Creative Commons license, and indicate if changes were made.

## References

1. Mawuenyega KG, Sigurdson W, Ovod V, Munsell L, Kasten T, Morris JC, Yarasheski KE, Bateman RJ (2010) Decreased clearance of CNS beta-amyloid in Alzheimer's disease. *Science* 330(6012):1774. <https://doi.org/10.1126/science.1197623>
2. Da Mesquita S, Louveau A, Vaccari A, Smirnov I, Cornelison RC, Kingsmore KM, Contarino C, Onengut-Gumuscu S et al (2018) Functional aspects of meningeal lymphatics in ageing and Alzheimer's disease. *Nature* 560(7717):185–191. <https://doi.org/10.1038/s41586-018-0368-8>
3. Ma Q, Zhao Z, Sagare AP, Wu Y, Wang M, Owens NC, Verghese PB, Herz J et al (2018) Blood-brain barrier-associated pericytes internalize and clear aggregated amyloid-beta42 by LRP1-dependent apolipoprotein E isoform-specific mechanism. *Mol Neurodegener* 13(1):57. <https://doi.org/10.1186/s13024-018-0286-0>
4. Tarasoff-Conway JM, Carare RO, Osorio RS, Glodzik L, Butler T, Fieremans E, Axel L, Rusinek H et al (2015) Clearance systems in the brain—implications for Alzheimer disease. *Nat Rev Neurol* 11(8):457–470. <https://doi.org/10.1038/nrneurol.2015.119>
5. Shinohara M, Tachibana M, Kanekiyo T, Bu G (2017) Role of LRP1 in the pathogenesis of Alzheimer's disease: Evidence from clinical and preclinical studies. *J Lipid Res* 58(7):1267–1281. <https://doi.org/10.1194/jlr.R075796>
6. Kanekiyo T, Cirrito JR, Liu CC, Shinohara M, Li J, Schuler DR, Shinohara M, Holtzman DM et al (2013) Neuronal clearance of amyloid-beta by endocytic receptor LRP1. *J Neurosci* 33(49):19276–19283. <https://doi.org/10.1523/JNEUROSCI.3487-13.2013>
7. Liu CC, Hu J, Zhao N, Wang J, Wang N, Cirrito JR, Kanekiyo T, Holtzman DM et al (2017) Astrocytic LRP1 mediates brain A $\beta$  clearance and impacts amyloid deposition. *J Neurosci* 37(15):4023–4031. <https://doi.org/10.1523/JNEUROSCI.3442-16.2017>
8. Urmoneit B, Prikulis I, Wihl G, D'Urso D, Frank R, Heeren J, Beisiegel U, Prior R (1997) Cerebrovascular smooth muscle cells internalize Alzheimer amyloid beta protein via a lipoprotein pathway: Implications for cerebral amyloid angiopathy. *Lab Invest* 77(2):157–166
9. Storck SE, Hartz AMS, Bernard J, Wolf A, Kachlmeier A, Mahringer A, Weggen S, Pahnke J et al (2018) The concerted amyloid-beta clearance of LRP1 and ABCB1/P-gp across the blood-brain barrier is linked by PICALM. *Brain Behav Immun* 73:21–33. <https://doi.org/10.1016/j.bbi.2018.07.017>
10. Pflanzner T, Janko MC, Andre-Dohmen B, Reuss S, Weggen S, Roebroek AJ, Kuhlmann CR, Pietrzik CU (2011) LRP1 mediates bidirectional transcytosis of amyloid-beta across the blood-brain barrier. *Neurobiol Aging* 32(12):2323 e2321–2323 e2311. <https://doi.org/10.1016/j.neurobiolaging.2010.05.025>
11. Shibata M, Yamada S, Kumar SR, Calero M, Bading J, Frangione B, Holtzman DM, Miller CA et al (2000) Clearance of Alzheimer's amyloid-ss(1–40) peptide from brain by LDL receptor-related protein-1 at the blood-brain barrier. *J Clin Invest* 106(12):1489–1499. <https://doi.org/10.1172/JCI10498>
12. Storck SE, Meister S, Nahrath J, Meissner JN, Schubert N, Di Spiezio A, Baches S, Vandenbroucke RE et al (2016) Endothelial LRP1 transports amyloid-beta(1–42) across the blood-brain barrier. *J Clin Invest* 126(1):123–136. <https://doi.org/10.1172/JCI81108>
13. Knauer MF, Orlando RA, Glabe CG (1996) Cell surface APP751 forms complexes with protease nexin 2 ligands and is internalized via the low density lipoprotein receptor-related protein (LRP). *Brain Res* 740(1–2):6–14
14. Kounnas MZ, Moir RD, Rebeck GW, Bush AI, Argraves WS, Tanzi RE, Hyman BT, Strickland DK (1995) LDL receptor-related protein, a multifunctional ApoE receptor, binds secreted beta-amyloid precursor protein and mediates its degradation. *Cell* 82(2):331–340



15. Pietrzik CU, Yoon IS, Jaeger S, Busse T, Weggen S, Koo EH (2004) FE65 constitutes the functional link between the low-density lipoprotein receptor-related protein and the amyloid precursor protein. *J Neurosci* 24(17):4259–4265. <https://doi.org/10.1523/JNEUROSCI.5451-03.2004>
16. Rebeck GW, Moir RD, Mui S, Strickland DK, Tanzi RE, Hyman BT (2001) Association of membrane-bound amyloid precursor protein APP with the apolipoprotein E receptor LRP. *Brain Res Mol Brain Res* 87(2):238–245
17. Ulery PG, Beers J, Mikhailenko I, Tanzi RE, Rebeck GW, Hyman BT, Strickland DK (2000) Modulation of beta-amyloid precursor protein processing by the low density lipoprotein receptor-related protein (LRP). Evidence that LRP contributes to the pathogenesis of Alzheimer's disease. *J Biol Chem* 275(10):7410–7415
18. Ulery PG, Strickland DK (2000) LRP in Alzheimer's disease: Friend or foe? *J Clin Invest* 106(9):1077–1079. <https://doi.org/10.1172/JCI11455>
19. Nalivaeva NN, Turner AJ (2013) The amyloid precursor protein: A biochemical enigma in brain development, function and disease. *FEBS Lett* 587(13):2046–2054. <https://doi.org/10.1016/j.febslet.2013.05.010>
20. De Strooper B, Annaert W (2010) Novel research horizons for presenilins and gamma-secretases in cell biology and disease. *Annu Rev Cell Dev Biol* 26:235–260. <https://doi.org/10.1146/annurev-cellbio-100109-104117>
21. Lillis AP, Van Duyn LB, Murphy-Ullrich JE, Strickland DK (2008) LDL receptor-related protein 1: Unique tissue-specific functions revealed by selective gene knockout studies. *Physiol Rev* 88(3):887–918. <https://doi.org/10.1152/physrev.00033.2007>
22. Li Y, Marzolo MP, van Kerkhof P, Strous GJ, Bu G (2000) The YXXL motif, but not the two NPXY motifs, serves as the dominant endocytosis signal for low density lipoprotein receptor-related protein. *J Biol Chem* 275(22):17187–17194. <https://doi.org/10.1074/jbc.M000490200>
23. Kwon OY, Hwang K, Kim JA, Kim K, Kwon IC, Song HK, Jeon H (2010) Dab1 binds to Fe65 and diminishes the effect of Fe65 or LRP1 on APP processing. *J Cell Biochem* 111(2):508–519. <https://doi.org/10.1002/jcb.22738>
24. Reekmans SM, Pflanzner T, Gordts PL, Isbert S, Zimmermann P, Annaert W, Weggen S, Roebroek AJ et al (2010) Inactivation of the proximal NPXY motif impairs early steps in LRP1 biosynthesis. *Cell Mol Life Sci* : CMLS 67(1):135–145. <https://doi.org/10.1007/s00018-009-0171-7>
25. Roebroek AJ, Reekmans S, Lauwers A, Feyaerts N, Smeijers L, Hartmann D (2006) Mutant Lrp1 knock-in mice generated by recombinase-mediated cassette exchange reveal differential importance of the NPXY motifs in the intracellular domain of LRP1 for normal fetal development. *Mol Cell Biol* 26(2):605–616. <https://doi.org/10.1128/MCB.26.2.605-616.2006>
26. Gordts PL, Reekmans S, Lauwers A, Van Dongen A, Verbeek L, Roebroek AJ (2009) Inactivation of the LRP1 intracellular NPxYxxL motif in LDLR-deficient mice enhances postprandial dyslipidemia and atherosclerosis. *Arterioscler Thromb Vasc Biol* 29(9):1258–1264. <https://doi.org/10.1161/ATVBAHA.109.192211>
27. Gordts PL, Bartelt A, Nilsson SK, Annaert W, Christoffersen C, Nielsen LB, Heeren J, Roebroek AJ (2012) Impaired LDL receptor-related protein 1 translocation correlates with improved dyslipidemia and atherosclerosis in apoE-deficient mice. *PLoS One* 7(6):e38330. <https://doi.org/10.1371/journal.pone.0038330>
28. Maier W, Bednorz M, Meister S, Roebroek A, Weggen S, Schmitt U, Pietrzik CU (2013) LRP1 is critical for the surface distribution and internalization of the NR2B NMDA receptor subtype. *Mol Neurodegener* 8:25. <https://doi.org/10.1186/1750-1326-8-25>
29. Rabiej VK, Pflanzner T, Wagner T, Goetze K, Storck SE, Eble JA, Weggen S, Mueller-Klieser W et al (2016) Low density lipoprotein receptor-related protein 1 mediated endocytosis of beta1-integrin influences cell adhesion and cell migration. *Exp Cell Res* 340(1):102–115. <https://doi.org/10.1016/j.yexcr.2015.11.020>
30. Martin AM, Kuhlmann C, Trossbach S, Jaeger S, Waldron E, Roebroek A, Luhmann HJ, Laatsch A et al (2008) The functional role of the second NPXY motif of the LRP1 beta-chain in tissue-type plasminogen activator-mediated activation of N-methyl-D-aspartate receptors. *J Biol Chem* 283(18):12004–12013. <https://doi.org/10.1074/jbc.M707607200>
31. Blanchard V, Moussaoui S, Czech C, Touchet N, Bonici B, Planche M, Canton T, Jedidi I et al (2003) Time sequence of maturation of dystrophic neurites associated with Abeta deposits in APP/PS1 transgenic mice. *Exp Neurol* 184(1):247–263
32. Dewachter I, Van Dorpe J, Smeijers L, Gilis M, Kuiperi C, Laenen I, Caluwaerts N, Moechars D et al (2000) Aging increased amyloid peptide and caused amyloid plaques in brain of old APP/V717I transgenic mice by a different mechanism than mutant presenilin1. *J Neurosci* 20(17):6452–6458
33. Jager S, Leuchtenberger S, Martin A, Czirr E, Wesselowski J, Dieckmann M, Waldron E, Korth C et al (2009) Alpha-secretase mediated conversion of the amyloid precursor protein derived membrane stub C99 to C83 limits Abeta generation. *J Neurochem* 111(6):1369–1382. <https://doi.org/10.1111/j.1471-4159.2009.06420.x>
34. DeMattos RB, Bales KR, Parsadanian M, O'Dell MA, Foss EM, Paul SM, Holtzman DM (2002) Plaque-associated disruption of CSF and plasma amyloid-beta (Abeta) equilibrium in a mouse model of Alzheimer's disease. *J Neurochem* 81(2):229–236
35. Pflanzner T, Petsch B, Andre-Dohmen B, Muller-Schiffmann A, Tschickardt S, Weggen S, Stütz L, Korth C et al (2012) Cellular prion protein participates in amyloid-beta transcytosis across the blood-brain barrier. *J Cereb Blood Flow Metab* 32(4):628–632. <https://doi.org/10.1038/jcbfm.2012.7>
36. Kanekiyo T, Liu CC, Shinohara M, Li J, Bu G (2012) LRP1 in brain vascular smooth muscle cells mediates local clearance of Alzheimer's amyloid-beta. *J Neurosci* 32(46):16458–16465. <https://doi.org/10.1523/JNEUROSCI.3987-12.2012>
37. Bell RD, Sagare AP, Friedman AE, Bedi GS, Holtzman DM, Deane R, Zlokovic BV (2007) Transport pathways for clearance of human Alzheimer's amyloid beta-peptide and apolipoproteins E and J in the mouse central nervous system. *J Cereb Blood Flow Metab* 27(5):909–918. <https://doi.org/10.1038/sj.jcbfm.9600419>
38. Games D, Adams D, Alessandrini R, Barbour R, Berthelette P, Blackwell C, Carr T, Clemens J et al (1995) Alzheimer-type neuropathology in transgenic mice overexpressing V717F beta-amyloid precursor protein. *Nature* 373(6514):523–527. <https://doi.org/10.1038/373523a0>
39. Zerbiniatti CV, Wozniak DF, Cirrito J, Cam JA, Osaka H, Bales KR, Zhuo M, Paul SM et al (2004) Increased soluble amyloid-beta peptide and memory deficits in amyloid model mice overexpressing the low-density lipoprotein receptor-related protein. *Proc Natl Acad Sci U S A* 101(4):1075–1080. <https://doi.org/10.1073/pnas.0305803101>
40. Pohlkamp T, Wasser CR, Herz J (2017) Functional roles of the interaction of APP and lipoprotein receptors. *Front Mol Neurosci* 10:54. <https://doi.org/10.3389/fnmol.2017.00054>
41. Zilberberg A, Yaniv A, Gazit A (2004) The low density lipoprotein receptor-1, LRP1, interacts with the human frizzled-1 (HFz1) and down-regulates the canonical Wnt signaling pathway. *J Biol Chem* 279(17):17535–17542. <https://doi.org/10.1074/jbc.M311292200>
42. Lillis AP, Mikhailenko I, Strickland DK (2005) Beyond endocytosis: LRP function in cell migration, proliferation and vascular permeability. *J Thromb Haemost* 3(8):1884–1893. <https://doi.org/10.1111/j.1538-7836.2005.01371.x>